Electrocatalytic reduction of oxygen and hydrogen peroxide at poly(*p*-aminobenzene sulfonic acid)-modified glassy carbon electrodes

S. Ashok Kumar, Shen-Ming Chen*

Department of Chemical Engineering and Biotechnology, National Taipei University of Technology, No. 1, Section 3, Chung-Hsiao East Road, Taipei 106, Taiwan, ROC

Abstract

The electrocatalytic ability of the modified electrodes for the reduction of dioxygen to hydrogen peroxide was investigated by using cyclic voltammetry and chronocoulometry techniques at poly(*p*-aminobenzene sulfonic acid) (PABS)-modified glassy carbon electrodes. The electrochemical reduction of oxygen (O_2) has been studied in pH 7.0 buffer solution by using PABS-modified glassy carbon rotating ring disk electrode (RRDE). The PABS-modified glassy carbon (GC) electrode (GC/PABS) showed excellent electrocatalytic activity for oxygen and hydrogen peroxide (H_2O_2) reduction reactions. The RRDE data indicated that the reduction of oxygen on GC/PABS electrodes proceeds by a two-electron pathway in aqueous buffer solution (pH 7.0). In addition, PABS-coated GC electrode was successfully utilized as an enzyme-less amperometric sensor for the detection of hydrogen peroxide (H_2O_2) in the range from 50 to 550 μM with detection limit of (S/N = 3) 10 μM.
© 2007 Elsevier B.V. All rights reserved.

Keywords: Hydrogen peroxide sensor; Electrocatalysis; Oxygen reduction; Polyaniline; Electro-active polymer

1. Introduction

Chemically modified electrodes (CMEs) have great significance as important analytical tools for the electrochemical determination of various analytes with the benefits of electrode modification. The modification of electrode results in efficient detection of electro-active biomolecules at very lower potential without its major interferences [1,2]. Generally, modification of electrodes surface was achieved by using inorganic and organic materials, among them polymer-modified electrodes (PMEs) are widely used [3]. Electropolymerization is a good approach to prepare PMEs as adjusting electrochemical parameters can control film thickness, permeation and charge transport characteristics. PMEs have many advantages in the detection of analytes because of its selectivity, sensitivity and homogeneity in electrochemical deposition, strong adherence to electrode surface and chemical stability of the film [4,5].

On the other hand, oxygen electrochemistry, particularly the reaction mechanism of oxygen reduction and the role of electrocatalyst in this reaction is one of the most important research area among the electrochemist since it has been one of the most important issues in the development of hydrogen–oxygen fuel cells, metal air batteries, industrial electrolytic process, electro-organic reactions, and fuel cells [6–9].

A survey of the literature report reveals that electrocatalytic reduction of O_2 using bare electrodes modified with anthroquinone derivative [10,11], polyaniline/nafion composite film [12], polyterthiophene carboxylic acid 1,5-diaminonaphthalene copper complex [13], gold nanoparticles dispersed into poly(aminothiophenol) [14], Pt/polyaniline [15], multi-walled carbon nanotubes/cobalt porphyrin-modified glassy carbon [16], carbon-supported RuSex nanoparticles with ultra-thin WO_3 films [17] and binary catalysts of Au nanoparticles/MnO_x nanoparticles [18] were reported and the electrocatalytic reduction of O_2 by water soluble iron porphyrin/phthalocyanines/porphyrins is also reviewed by Kobayashi and Nevin [19]. Electrocatalytic reduction reaction of molecular O_2 has been studied at metal, metal nanoparticles or metal-sited ligands due to their

* Corresponding author. Tel.: +886 2 27017147; fax: +886 2 27025238.
 E-mail address: smchen78@ms15.hinet.net (S.-M. Chen).

catalytic reduction of O_2 at reduced over potential but the main disadvantage of those methods are cost of the electrocatalyst. Thus, numerous efforts have been paid to the search for cheaper materials with excellent electrocatalytic activity towards the oxygen reduction reaction (ORR) to replace the costly metal (Pt)-based electrocatalysts.

On the other side, conducting polymers have potential applications in various fields such as fuel cells, biosensors, electroanalysis, electrocatalysis, electrochromic displays and others [3,8,9]. The ORR at electronically conducting polymers (ECPs) such as polyaniline (PANI), polypyrrole, polythiophen, poly(3-methyl)thiophen and poly(3,4-ethylenedioxythiophene) (PEDOT)-modified electrodes have been studied [20]. Interestingly, their results suggested that electrochemical investigations of above ECPs-modified electrodes in oxygen-saturated electrolytes indicated that existence of electrocatalytic activity towards the ORR with the exception of PEDOT [20].

Among ECPs, PANI and its derivatives have been the focus of much attention. Sulfonated polyaniline (SPAN) is of interest because of its unusual physical properties, improved processability, and potential industrial applications [21,22]. The solubility of polyaniline in aqueous solutions and in most common organic solvents is greatly improved by the presence of $-SO_3{}^-$ groups [23]. The environmental stability of the parent polyaniline is also further improved in SPAN. The conductivity of SPAN is independent of external protonation in a broad pH range. SPAN was found to have better thermal stability than its parent polyaniline [24]. SPAN is electrochemically active in wide pH range 1–12 rather than PANI. We have been reported the electrochemical polymerization of p-aminobenzene sulfonic acid doped with flavins and its electrochemical properties [25].

To the best of our knowledge, for the first time in this paper, we report the electrocatalytic reduction reaction of molecular oxygen and H_2O_2 at substituted polyaniline-modified electrodes. The effect of potential, pH, scan rate and film thickness of PABS polymer on O_2 reduction and stability of the PMEs were discussed. RRDE is sued to study the electrode kinetics. Moreover, the PABS-modified electrode was utilized as a sensor for the detection of H_2O_2 in physiological condition.

2. Experimental

2.1. Reagents and equipment

All chemicals and reagents used in this work were of analytical grade and were used as received without further purification. Those were hydrogen peroxide (∼30%) solution and p-aminobenzene sulfonic acid were purchased from Sigma–Aldrich (St. Louis, MO, USA). Sulfuric acid (H_2SO_4) and sodium hydroxide (NaOH) were purchased from Wako pure chemicals (Osaka, Japan). Sodium acetate (CH_3COONa) and sodium dihydrogen phosphate (NaH_2PO_4) were received from E-Merck (Darmstadt, Germany).

Supporting electrolytes used for electrochemical experiments were 0.1 M H_2SO_4 (pH 1.0), 0.1 M H_2SO_4 + 0.1 M NaOH (for pH 2.0–3.0), 0.2 M CH_3COOH + 0.2 M CH_3COONa (for pH 4.0–5.0) and 0.1 M NaH_2PO_4 + 0.1 M NaOH (for pH 6.0–12.0).

The required values of pH solutions were obtained with the described solutions by mixing and the pH of the medium was measured using a Suntex Model SP-701 pH meter (Jiangsu, China). The aqueous solutions were prepared by using doubly distilled deionized water and before each experiment the solutions were deoxygenated by purging with pre-purified nitrogen gas with an exception of O_2 reduction reactions.

Electrochemical measurements were performed with CH Instruments (TX, USA) Model-400 potentiostat with conventional three-electrode cell. A BAS glassy carbon and platinum wire are used as the working electrode and counter electrode, respectively. All the cell potentials were measured with respect to an Ag/AgCl [KCl (sat)] reference electrode. Hydrodynamic voltammetric studies on dioxygen reduction reaction were performed on a Bi-potentiostat Model CHI750A (TX, USA) having an analytical rotator model AFMSRK with MSRX speed control (PINE Instruments, USA). All experiments were carried out at room temperature.

2.2. Electrode modification

Prior to use, the working electrodes were mechanically polished with alumina powder (Al_2O_3, 0.05 μm) up to a mirror finish. Then the electrodes were cycled in 0.2 M sulfuric acid in a potential range from −0.5 to 1 V at a sweep rate of 100 mV s^{-1} until a stable voltammogram obtained. The electrochemical deposition of PABS films were carried out by cyclic voltammetry (between −0.5 and 2.0 V at 100 mV s^{-1}) for 30 cycles. The electropolymerization was conducted in a three-electrode cell with glassy carbon as the working electrode, Ag/AgCl as the reference electrode and platinum wire as the counter electrode. The electrolyte consisted of 2 mM p-aminobenzene sulfonic acid monomer in aqueous solution of 0.1 M HNO_3. The resulting films were washed with doubly distilled deionized water before proceed electrochemical measurements. Finally, the modified GC/PABS electrode was electroactivated by cyclic voltammetry from −0.75 to 0.65 V in pH 7.0 buffer solutions at a scan rate of 100 mV s^{-1} and then electrochemical properties of the GC/PABS were studied. The electrochemical polymerization mechanism of p-aminobenzene sulfonic acid in acidic solution was previously well studied and reported by many authors [21–25].

3. Results and discussion

3.1. Electrochemical behavior of GC/PABS film-modified electrodes

The cyclic voltammograms (CVs) were recorded by using GC/PABS-modified electrode in aqueous buffer solutions (pH 7.0) at different scan rates; it was showed one obvious reversible redox couple centered at formal potential ($E^{0'}$) 0.04 V versus Ag/AgCl electrode. The anodic and cathodic peak currents were directly proportional to the scan rate in the range of 10–100 mV s^{-1} which is an indication of a surface confined redox process. According to the equation, $I_p = n^2F^2\Gamma A\upsilon/4RT$ and $Q_\Gamma = nFA\Gamma$ where n is the number of electrons, A the work-

ing electrode area ($0.0707\,cm^2$), υ scan rate ($10\,mV\,s^{-1}$) and other parameters have their usual meanings [26,27], the electron transfer number and the surface coverage were calculated to be 1.85 and 5.866×10^{-10} mol/cm², respectively.

The effect of external solution pH on the response of GC/PABS was investigated in the pH range of 1–12. It was found that both the cathodic and anodic peak potentials shifted to negative direction with increasing pH of the electrolyte solution. The $E^{0'}$ versus pH plot yields straight line with a slope of 57 mV per unit change in solution pH which was very close to the anticipated Nernstian value for equal number of protons and electrons transfer reaction. It suggests that the overall redox reaction of the polymer film comprises a two-electron and two-proton process.

On the other hand the anodic peak potentials shifted to the positive direction and the cathodic peak potentials shifted to the negative direction at higher scan rate ($\upsilon > 100\,mV\,s^{-1}$), which resulted in an increase of the peak separation between anodic and cathodic peak. The peak separation at higher scan rate could be used to estimate the heterogeneous electron transfer rate constant. According to the method of Laviron [28,29] the electron transfer rate constant (k_s) value can be determined by measuring the variation of peak potential with scan rate. The values of peak potentials were proportional to the logarithm of the scan rate higher than $0.5\,V\,s^{-1}$ (Fig. 1). The slope value of the ΔE_{pc} versus $log(\upsilon)$ was about $-214\,mV$ for GC/PABS-modified electrode. Using the equation $E_p = K - 2.3030(RT/\alpha nF) log(\upsilon)$ and the two electrons transferred for polymer redox peak a charge transfer coefficient (α) 0.8 was obtained, introducing these values in Eq. (1), an apparent surface k_s value $1.6\,s^{-1}$ was estimated.

$$\log K_s = \alpha \log(1-\alpha) + (1-\alpha)\log\alpha - \log(RT/nF\upsilon)$$
$$- \alpha(1-\alpha)\frac{nFE}{2.3RT} \tag{1}$$

3.2. Electrocatalytic dioxygen reduction reaction

Fig. 2 shows the CVs of buffer solution (pH 7.0) saturated with nitrogen (curve a) and with O_2-saturated buffer solution
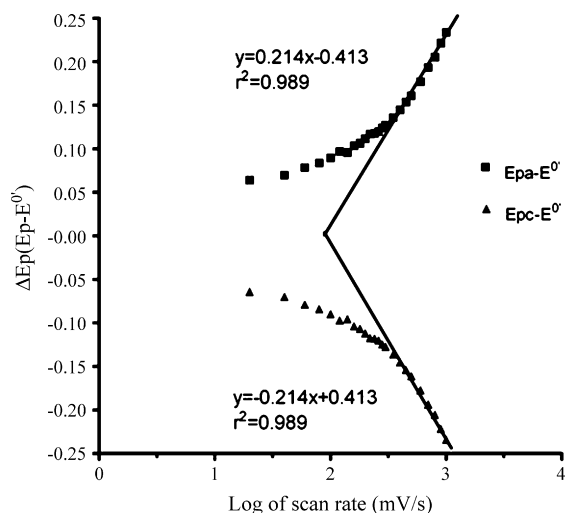

Fig. 1. Plot of peak potential separation vs. log υ for GC/PABS films.

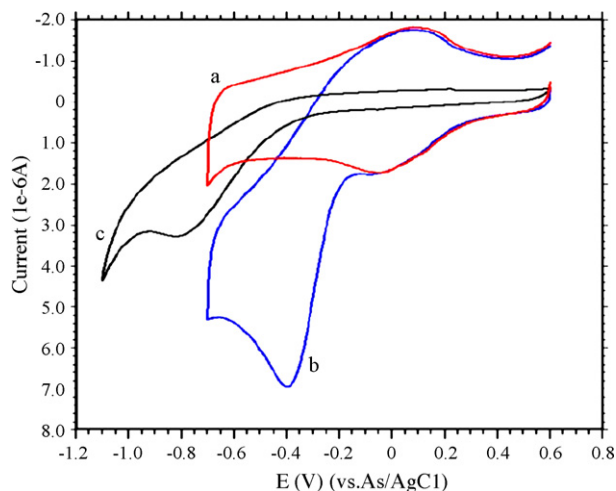Fig. 2. CVs of GC/PABS-modified electrodes in pH 7.0 PBS: (a) N_2-saturated solution; (b) O_2-saturated solution and (c) bare GC electrode in O_2 saturated solution. Scan rate $20\,mV\,s^{-1}$.

(curve b) at the GC/PABS-modified electrode. In the absence of O_2, the cyclic voltammogram is the same as that shown in Fig. 2, curve a. In the presence of O_2 a new cathodic peak was developed about $-390\,mV$ at a scan rate of $20\,mV\,s^{-1}$. This cathodic peak corresponds to the electrochemical reduction reaction of O_2 at the GC/PABS electrode (Fig. 2, curve b). The electrochemical reduction of O_2 at a bare GC electrode shows a broad and ill-defined cathodic peak (Fig. 2, curve c) and the cathodic peak potential is located at $-830\,mV$ at a scan rate of $20\,mV\,s^{-1}$. Based on the above results, it was concluded that GC/PABS electrode reduced the overpotential required for O_2 reduction about 440 mV. Furthermore, the peak currents of curve c are much less than that in Fig. 2, curve b. All the above results indicated that the GC/PABS electrode has excellent electrocatalytic activity for the electrochemical reduction reaction of O_2.

3.3. The effect of pH and scan rate

To ascertain the effect of pH on the electrocatalytic reduction of dioxygen at a GC/PABS was examined in the pH range between 1.0 and 12.0 using cyclic voltammetry. The reduction peak potential of oxygen and the formal potential ($E^{0'}$) of reversible redox peak PABS are found to be pH-dependent. However, PABS redox peak was shifted to negative potential with respect to pH of the contacting solution, cathodic peak potential of O_2 reduction found to be unequal due to the differences in their kinetic behavior. On the other side, there is a gradual increase in the cathodic peak current for O_2 reduction with increasing pH of the buffer solution up to 7.0. Maximum enhancement of cathodic current and shift in oxygen reduction potential at the GC/PABS-modified electrode led to the selection of pH 7.0 as an optimum condition to investigate the electrocatalysis of oxygen reduction reaction.

To investigate the effect of scan rate on O_2 reduction reaction at GC/PABS in oxygen-saturated solutions CVs were recorded. The variation of cathodic peak current with scan rate was shown

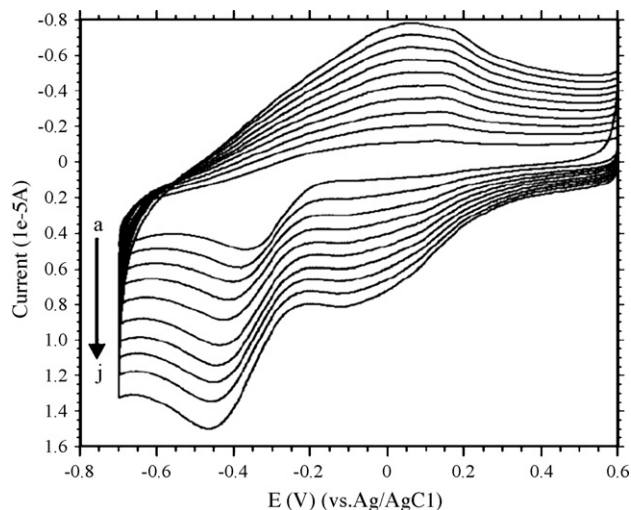Fig. 3. CVs of GC/PABS-modified electrode in O_2-saturated pH 7.0 PBS at different scan rates. The scan rates from inner to outer are 10–100 mV s^{-1}.

Fig. 4. Chronocoulomogram of GC/PABS at pH 7.0 in (a) presence, (b) absence of oxygen and (c) bare GC electrode in O_2 saturated solution.

in Fig. 3. The cathodic peak current, I_{pc}, varies linearly with the square root of scan rate, $\upsilon^{1/2}$. This indicates that the oxygen reduction process is diffusion controlled.

To study the effect of positive potential used for electro-polymerization of p-aminobenzene sulfonic acid on catalytic current and cathodic peak potential of O_2 reduction reaction was carried out. The obtained results are presented in Table 1. The catalytic current was increased whereas E_{pc} for O_2 reduction was moved towards more positive potential with respect to the anodic potential range used for polymerization. Beyond 2 V, there is almost no change was observed in catalytic current as well as in E_{pc} for O_2 reduction at GC/PABS. For this reason, anodic potential 2 V is selected an optimum for electro-polymerization of p-aminobenzene sulfonic acid to prepare GC/PABS electrode for electrocatalytic reduction reaction of oxygen.

3.4. Chronocoulometry

The chronocoulometric behavior of GC/PABS-modified electrode was examined by the double potential-step technique in the absence and presence of oxygen with the same initial and final potentials. As an example, Fig. 4 exhibits the chronocoulomogram of GC/PABS. In oxygenated buffer, a large enhancement of charge and the appearance of a nearly flat line on reversal of the potential indicate the irreversible electrocatalytic reduction of oxygen. The number of electrons (n) involved in oxygen reduction at the modified electrode is evaluated from the
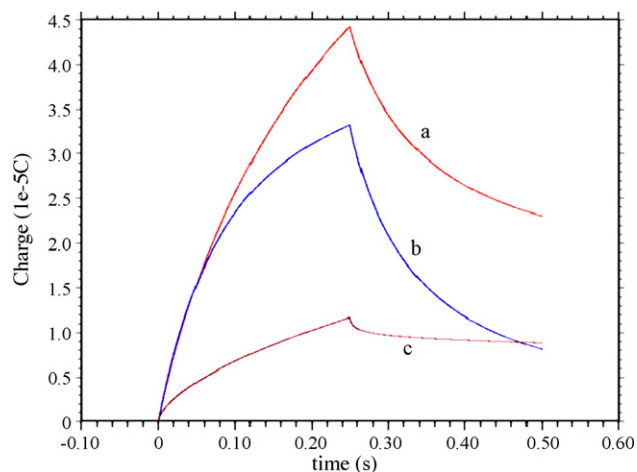
slope of Q versus $t^{1/2}$ plots under oxygen-saturated conditions, using the Cottrell equation, i.e.,

$$Q = 2nFACD^{1/2}\pi^{-1/2}t^{1/2} \qquad (2)$$

where $C = 1.25$ mM, $A = 0.0707$ cm^2 and $D = 2.1 \times 10^{-5}$ cm^2 s^{-1}. The calculated n value is 2.07. Hence, the reduction product is hydrogen peroxide [10,11,30].

3.5. Rotating ring disc voltammetry

Hydrodynamic voltammetric studies were also performed on rotating GC disk electrodes modified with PABS in the absence and presence of oxygen in pH 7.0 buffer solution to determine the kinetic parameters more quantitatively. As an illustration, Fig. 5A represents a set of current–potential curves in an oxygen-saturated buffer of pH 7.0 at various angular velocities, ω, with a rotating disk GC electrode modified with PABS. Curve (a$'$) is the response of the modified electrode in the absence of oxygen. The limiting current, I_l, is defined as the difference between the currents on a modified electrode at the potential corresponding to the diffusion plateau in deaerated and O_2-saturated solutions. The Levich and Koutecky–Levich plots are formulated from the limiting currents measured at a potential −800 mV and are given in Fig. 5B and C, respectively.

The Levich plot in Fig. 5B is very close to the theoretically calculated line for a two-electron process ($n = 2$) and exhibits a linear relationship between limiting current and rotation rate (ω) values. And, the corresponding Koutecky–Levich

Table 1
The effect of applied potential on the surface coverage of PABS, catalytic current and E_{pc} of O_2 reduction

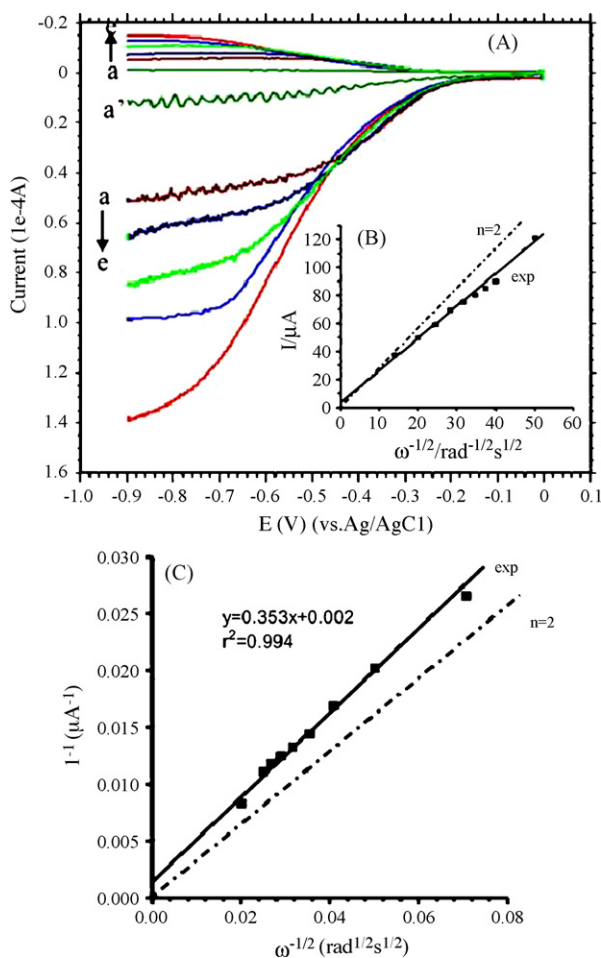| Applied potential used for polymerization (V)	Polymer surface coverage, Γ ($\times 10^{-10}$ mol/cm^2)	E_{pc} for O_2 reduction (V)	Catalytic current, I_{pc} ($\times 10^{-6}$ A)
1.2	2.1462	−0.764	4.606
1.4	2.8388	−0.673	4.890
1.6	3.8190	−0.600	5.159
1.8	4.6610	−0.539	6.031
2.0	5.8660	−0.390	7.587
2.2	5.8059	−0.401	6.812

Fig. 5. A Current–potential curves for reduction of oxygen (1.25 mM) at rotating ring (Pt) glassy carbon disk electrode modified with PABS in pH 7.0 solution at various rotation rates (rpm) (scan rate of 10 mV s^{-1}). B Levich plot of limiting currents at −800 mV (exp), and theoretical Levich plots for two ($n = 2$) electron reduction reaction of O_2. C Koutecky–Levich plots of above data.

plot (Fig. 5C) also shows a linear relationship between I^{-1} and ω^{-1} with a slope close to that of the theoretical line for two-electron reduction reaction of oxygen. These findings suggest that adsorbed polymer film sustains the reduction of oxygen to H_2O_2. The heterogeneous rate constant for the catalytic oxygen reduction reaction can be evaluated from the intercept of the Koutecky–Levich plot using the expression [10,11,31]:

$$I_l^{-1} = I_k^{-1} + I_{lev}^{-1} \quad (3)$$

$$I_k = nFAK_{O_2}C_{O_2}\Gamma_{PABS} \quad (4)$$

where Γ_{PABS} indicates the surface coverage of electro-active polymer on GC disk electrode. The surface coverage Γ_{PABS} can be evaluated from the equation $\Gamma = Q/nFA$, where Q is the charge obtained by integrating the cathodic peak under the background correction at low scan rate of 10 mV s^{-1} and the other symbols have their usual meanings.

$$I_l^{-1} = [nFAkC_{O_2}\Gamma]^{-1} + [0.62nFAD_{O_2}^{2/3}\gamma^{-1/6}\omega^{1/2}C_{O_2}]^{-1} \quad (5)$$

Therefore, the kinetic parameters can be evaluated using Koutecky–Levich plots (Fig. 5C) that are analyzed according

to Eq. (5). The intercepts of the Koutecky–Levich plots in Fig. 5C correspond to a reciprocal kinetic current I_k^{-1}, which describes the current limited by the rate of the electrocatalytic reaction and from which K_{O_2} can be obtained directly [30,31]. The values of the heterogeneous rate constant for the reduction of O_2, K_{O_2} at the surface of PABS is obtained from Eq. (4) where $n = 2$, F is the Faraday's constant (96 485 C mol^{-1}), A the effective area of the electrode (0.16 cm^2), C_{O_2} indicates the concentration of O_2 in oxygen saturated solution (1.25 mM) and Γ_{PABS} refers to the electrode surface coverage (1.262 × 10^{-10} mol/cm^2) of GC/PABS disk electrode. The heterogeneous rate constant and diffusion coefficient of O_2 in buffered aqueous O_2-saturated solution were determined to be 2.55 × 10^{-3} M^{-1} s^{-1} and (1.95 ± 0.05) × 10^{-5} using the Levich plot. The value of kinematic viscosity of water υ used in this calculation was 0.01 cm^2 s^{-1}. The value obtained for D_{O_2} is good comparable with other reported values elsewhere [10,11,30,31].

In Fig. 5A, it was observed that O_2 reduction current at the GC disk electrode and the oxidation current of H_2O_2 at platinum ring electrode (potential held at +0.7 V) increased with the increase of rotation rate. The product generated at the disk is collected at the ring. The collection efficiency (N) was calculated from the ratio between the ring current (I_R) and disk current (I_D) [26]. The I_R/I_D was found to be 0.12, that is, 12% of the product generated at the disk is collected at the ring. Our experiments as well as previous literature report [20] revealed that the following probable mechanism for oxygen reduction reaction at PABS-coated electrode (Scheme 1):

$$(PABS)_{oxd} + nH^+ + ne \leftrightarrow (PABS)_{red} \quad (6)$$

$$(PABS)_{red} + nO_2 \rightarrow (PABS)_{oxd} + nH_2O_2 \quad (7)$$
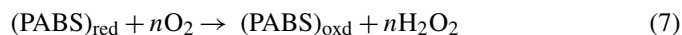
3.6. H_2O_2 detection using cyclic voltammetry and amperometry

The determination of H_2O_2 concentrations is very important in clinical, biological and chemical samples, as well as in food processing and fermentation process [32,33]. Among the many techniques, electrochemical methods such as amperometric sensor has several advantages including low cost, ease handling, operational stability and suitability for real-time analysis. Most of the amperometric sensor reported for H_2O_2 detection
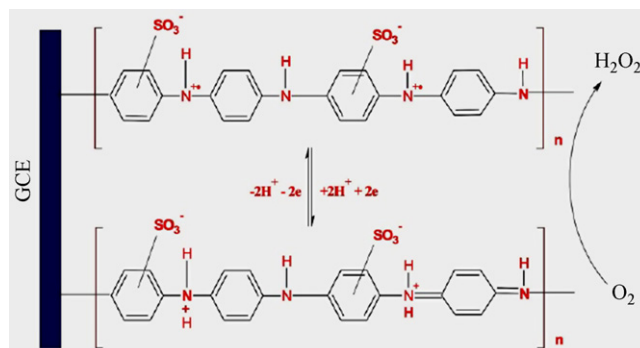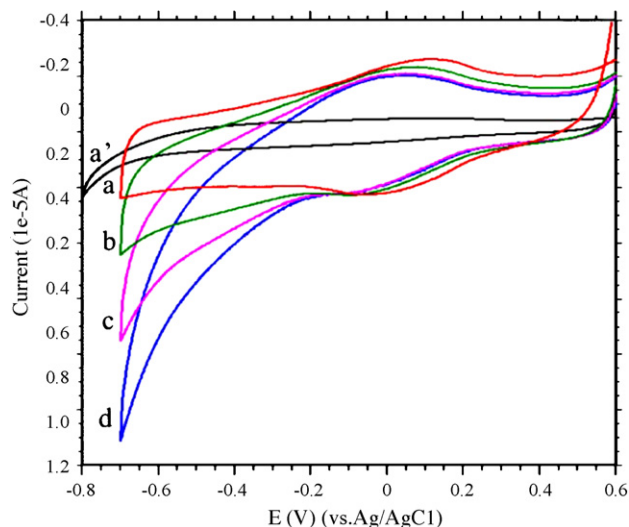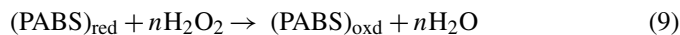

Scheme 1.

Fig. 6. CVs of GC/PABS-modified electrodes in pH 7.0 PBS—H_2O_2: (a) 0.0 μM, (b) 100 μM, (c) 200 μM, (d) 300 μM and (a′) bare GC electrode with 300 μM H_2O_2; scan rate 20 mV s^{-1}.

mainly based on enzymes [32] and heme proteins [34–36]. The feasibility of utilizing PABS polymer-coated electrode as an amerometric sensors was tested in this context.

In order to test the electrocatalytic activity of GC/PABS-modified electrode for the electrochemical reduction of H_2O_2, the CVs were obtained at various concentrations of H_2O_2 in pH 7.0 buffer solution as shown in Fig. 6. In the absence of H_2O_2, however, the polymer exhibited a redox couple at $E^{0'}$ 0.04 V (Fig. 6a). Upon the addition of 100, 200 and 300 μM H_2O_2 (Fig. 6b–d), there was a drastic and linear increase in the cathodic peak current at −0.7 V was observed. This phenomenon indicated that the GC/PABS effectively reduced the H_2O_2. The cathodic current further increased linearly with respect to the added concentration of H_2O_2, in contrast bare GC electrode did not reveal any signal for H_2O_2 over the potential range studied (Fig. 6a′).

The voltammetric data detailed above suggested that GC/PABS-modified electrode facilitates the low potential amperometric detection of H_2O_2. Amperometric study (Fig. 7A) examines this possibility by comparing the current–time tracings at −0.7 V using GC/PABS-modified electrode to successive additions of 50 μM H_2O_2. As expected from the voltammetric profiles, the GC/PABS sensor responds favorably to each addition yielding steady-state signals within 5 s. These data indicated that the GC/PABS electrode has a higher electrocatalytic activity for H_2O_2. Analysis of the amperometric responses and the standard addition data showed that limit of detection is 10 μM (S/N = 3); the linear range was observed in the range of 50–550 μM, after this range the current attained steady state (Fig. 7B). In addition, GC/PABS electrode displayed good reproducibility with a relative standard deviation of 4.2% for seven independent determinations in 100 μM H_2O_2 solution. Moreover, the current depended linearly with square root of scan rate in the range of 10–100 mV s^{-1}, suggesting a reaction controlled by diffusion-controlled process on GC/PABS electrode. This observation is similar to that reported elsewhere [19,20]. The

proposed mechanism for the reduction of H_2O_2 by PABS is as follows:

$$(PABS)_{oxd} + nH^+ + ne \leftrightarrow (PABS)_{red} \quad (8)$$

$$(PABS)_{red} + nH_2O_2 \rightarrow (PABS)_{oxd} + nH_2O \quad (9)$$

The CVs obtained for a series of H_2O_2 solutions with various concentrations are illustrated in Fig. 7. From Fig. 7 it can be seen that the reduction current responses increased with increasing the H_2O_2 concentration. Thus, the GC/PABS electrode can be used as an amperometric sensor for determination of H_2O_2 in solution.

Kobayashi et al. [37] reported that the catalytic activity of parent PANI is limited by the pH value, since PANI has little electrochemical activity at pH > 4; the potential range of the electroactivity for PANI decreases with increasing pH value and its redox
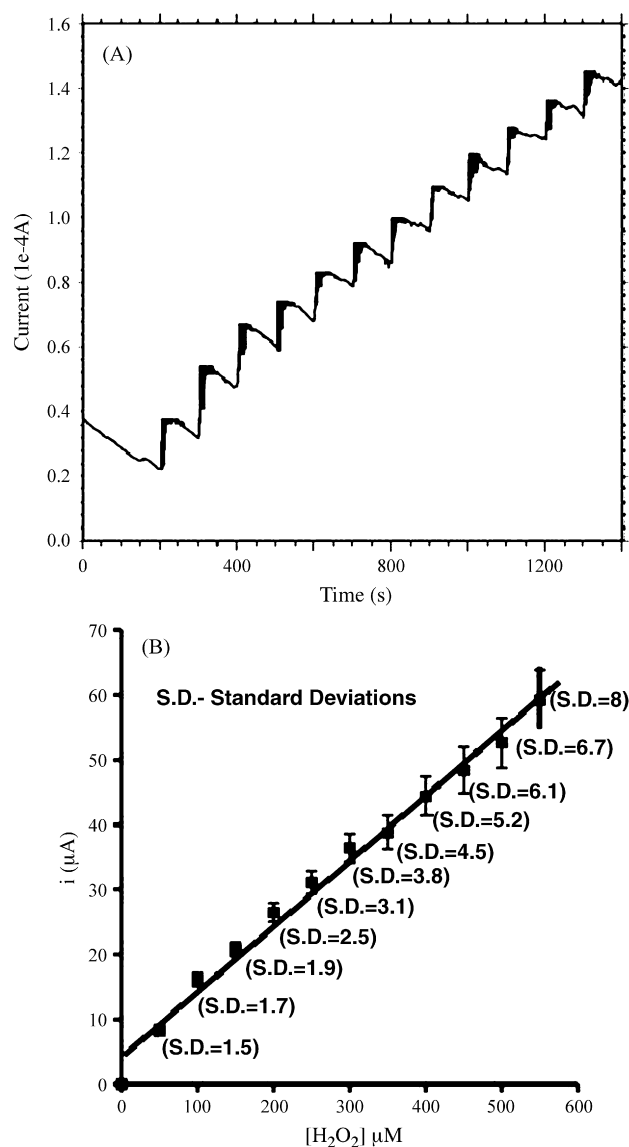

Fig. 7. Typical amperometric curve obtained with a GC/PABS electrode in pH 7.0 PBS at an applied potential of −0.7 V s^{-1} vs. Ag/AgCl, stirring rate ∼500 rpm (A) successive additions of 50 μM H_2O_2 solution and (B) the corresponding standard addition plots (each value is the mean of three measurements).

peaks disappear in the cyclic voltammetry for pH > 5. Thus, in general, the redox potential of species to be oxidized and reduced by PANI is within the potential range in which PANI itself is electroactive, restricts its application in electrocatalysis. Recently, Santhosh et al reported a PANI grafted on multi-walled carbon nanotube-modified electrode as an amperometric sensor for H_2O_2 determination [38] and they also found that PANI-coated GC electrode is not suitable for determination of H_2O_2. Based on our experimental results and earlier reports [37,38] we have concluded that our proposed new modified electrode (GC/PABS) can be much useful for determination of H_2O_2 in neutral pH environment than its parent polyaniline-modified electrode.

3.7. Stability test of the modified electrodes

Finally, the stability of the GC/PABS-modified electrode was evaluated by cycling 500 times in the potential range between -0.7 and 0.6 V at a scan rate of $100\,\mathrm{mV\,s^{-1}}$ in pH 7.0 buffer solution. It is observed that redox peak current of PABS remained stable on continuous cycling even more than 500 cycles. Good stability of the modified electrode may reflect the irreversible deposition of PABS on GC electrode. Based on the above results, it was concluded that GC/PABS-modified electrode have good stability and also time required for electrode fabrication is less than 10 min so it can be prepared whenever needed.

4. Conclusions

For the first time in this paper, electro-polymerized-substituted polyaniline derivative was used to modify GC electrode for the electrocatalytic reduction of O_2 and H_2O_2. The electrocatalytic properties of modified electrode were studied by using cyclic voltammetry, chronocoulometry and RRDE. PABS was strongly and irreversibly adsorbed onto GC electrode surface. The modified GC/PABS exhibited potent electrocatalytic activities towards dioxygen reduction in pH 7.0 buffer solutions with a reduced overpotential of about $440\,\mathrm{mV}$ lower than plain GC electrode. The kinetic parameters such as electrocatalytic reaction rate constant and diffusion coefficient of dioxygen were evaluated from rotating ring disk voltammetric measurements. Moreover, GC/PABS electrode was successfully used as an enzyme-less amperometric sensor for detection of H_2O_2 in the range from 50 to $550\,\mu M$. The detection limit was found to be $10\,\mu M$ (S/N = 3).

Acknowledgements

References

[1] R.W. Murray, in: A.J. Bard (Ed.), Electroanalytical Chemistry, vol. 13, Marcel Dekker, New York, 1984, pp. 191–368.

[2] E. Laviron, in: A.J. Bard (Ed.), Electroanalytical Chemistry, vol. 12, Marcel Dekker, New York, 1982, pp. 53–157.

[3] A. Malinauskas, J. Malinauskienė, A. Ramanavičius, Nanotechnology 16 (2005) R51–R62.

[4] S. Cosnier, Anal. Bioanal. Chem. 377 (2003) 507–520.

[5] L. Xu, W. Chen, A. Mulchandani, Y. Yan, Angew. Chem. Int. Ed. 44 (2005) 6009–6012.

[6] K. Kinoshita, Electrochemical Oxygen Technology, Wiley, New York, 1992.

[7] S. Mukerjee, in: A. Wieckowski, E.R. Savinova, C.G. Vayenas (Eds.), Catalysis and Electrocatalysis at Nanoparticle Surfaces, Marcel Dekker, New York, 2003, p. 501.

[8] G. Kossmehl, G. Engelmann, in: D. Fichou (Ed.), Handbook of Oligo and Polythiophenes, Wiley–VCH, New York, 1999 (Chapter 10).

[9] C. Lamy, J.M. Leger, F. Garnier, in: H.S. Nalwa (Ed.), Handbook of Organic Conductive Molecules and Polymers, vol. 3, John Wiley & Sons, New York, 1997 (Chapter 10).

[10] P. Manisankar, A. Gomathi, Electroanalysis 17 (2005) 1051–1057.

[11] P. Manisankar, A. Gomathi, J. Power Sources 150 (2005) 240–246.

[12] Q. Yang, Y. Wang, H. Nakano, S. Kuwabata, Polym. Adv. Technol. 16 (2005) 759–763.

[13] M. Boopathi, M.-S. Won, Y.H. Kim, S.C. Shin, Y.-B. Shim, J. Electrochem. Soc. 149 (2002) E265–E271.

[14] A.I. Gopalan, K.-P. Lee, K.M. Manesh, P. Santhosh, J. Heon Kim, J. Mol. Catal. A: Chem. 256 (2006) 335–345.

[15] C. Coutanceau, M.J. Croissant, T. Napporn, C. Lamy, Electrochim. Acta 46 (2000) 579–588.

[16] J. Qu, Y. Shen, X. Qu, S. Dong, Electroanalysis 16 (2004) 1444–1450.

[17] P.J. Kulesza, K. Miecznikowski, B. Baranowska, M. Skunik, S. Fiechter, P. Bogdanoff, I. Dorbandt, Electrochem. Commun. 8 (2006) 904–908.

[18] M.S. El-Deaba, T. Ohsaka, J. Electrochem. Soc. 153 (2006) A1365–A1371.

[19] N. Kobayashi, W.A. Nevin, Appl. Organomet. Chem. 10 (1996) 579–590.

[20] V.G. Khomenko, V.Z. Barsukov, A.S. Katashinskii, Electrochim. Acta 50 (2005) 1675–1683.

[21] J. Yue, A.J. Epstein, J. Am. Chem. Soc. 112 (1990) 2800–2801.

[22] J. Yue, Z.H. Wang, K.R. Cromack, A.J. Epstein, A.G. MacDiarmid, J. Am. Chem. Soc. 113 (1991) 2665–2671.

[23] S. Shimizu, T. Saitoh, M. Uzawa, M. Yuasa, K. Yano, T. Maruyama, K. Watanabe, Synth. Met. 85 (1997) 1337–1338.

[24] J. Yue, A.J. Epstein, Z. Zhong, P.K. Gallogher, A.G. MacDiarmid, Synth. Met. 41 (1991) 765–768.

[25] S.A. Kumar, S.M. Chen, Sensor Actuator B: Chem. 123 (2007) 964–977.

[26] A.J. Bard, L.R. Faulkner, Electrochemical Methods Fundamentals and Applications, Wiley, New York, 1980, pp. 521–525.

[27] A.P. Brown, F.C. Anson, Anal. Chem. 49 (1977) 1589–1595.

[28] E. Lavion, J. Electroanal. Chem. 101 (1979) 19–28.

[29] E. Laviron, J. Electroanal. Chem. 52 (1974) 355–393.

[30] A. Salimi, H. Eshghi, H. Sharghi, S.M. Golabi, M. Shamsipur, Electroanalysis 11 (1999) 114–119.

[31] S. Golabi, J.B. Raoof, J. Electroanal. Chem. 416 (1996) 75–82.

[32] B. Šljukić, C.E. Banks, C. Salter, A. Crossley, R.G. Compton, Analyst 131 (2006) 670–677.

[33] D.R.S. Jeykumari, S.S. Narayanan, Nanotechnology 18 (2007) 125501.

[34] S.A. Kumar, S.M. Chen, Biosens. Bioelectron. 22 (2007) 3042–3050.

[35] S.A. Kumar, S.M. Chen, Talanta 72 (2007) 831–838.

[36] A. Härtl, E. Schmich, J.A. Garrido, J. Hernando, S.C.R. Catharino, S. Walter, P. Feulner, A. Kromka, D. Steinmüller, M. Stutzmann, Nat. Mater. 3 (2004) 736–742.

[37] T. Kobayashi, N. Yoneyama, H. Tamura, J. Electroanal. Chem. 177 (1984) 281–291.

[38] P. Santhosh, K.M. Manesh, A. Gopalan, K.-P. Lee, Anal. Chim. Acta 575 (2006) 32–38.